International Journal of GEOMATE, Oct., 2022, Vol.23, Issue 98, pp.84-91
ISSN: 2186-2982 (P), 2186-2990 (O), Japan, DOI: https://doi.org/10.21660/2022.98.3461
Geotechnique, Construction Materials and Environment

SHAFT RESISTANCE MECHANISM FOR PILES CLOSE TO BACKFILLED SAND AND ITS EVALUATION

* Hiroshi Nagai [1], and Kenta Nakamura [2]

[1] College of Design and Manufacturing Technology, Muroran Institute of Technology, Japan
[2] Division of Sustainable and Environmental Engineering, Graduate School of Engineering, Muroran Institute of Technology, Japan

*Corresponding Author, Received: 23 May 2022, Revised: 20 August. 2022, Accepted: 09 Oct. 2022

ABSTRACT: In this paper, compressive loading tests of a pile overlapping backfilled soil of different densities in a part of the surrounding soil were conducted to quantify the shaft resistance of the pile and the shear failure behavior of the soil adjacent to the pile. In particular, several layers of colored sand were placed in the model soil to focus on the location of shear failure in the soil near the pile. The thickness of the shear band that contributed to the shaft resistance of the pile was investigated based on the deformation of the colored sand layer observed after the loading test. In addition, a method for evaluating the increase in horizontal earth pressure due to the settlement of the pile based on cavity expansion theory was investigated. A calculation method for pile shaft resistance that considers backfilled soil was developed. The validity of the calculation method was confirmed through a comparison with experimental results.

Keywords: New pile, Backfilled soil, Pile shaft resistance, Shear band, Soil dilatancy, Loading test

1. INTRODUCTION

When an old structure is reconstructed, existing old foundations are sometimes reused, but in many cases, they are still dismantled and removed. When old piles are removed, their holes should, in principle, be backfilled to match the conditions of the surrounding ground. However, the backfilled material may have diverse physical properties or maybe in a condition different from that of the surrounding ground. New piles are often installed near the backfilled material. The mismatch between the backfilled material and surrounding soil may affect the bearing performance of new piles, especially the shaft resistance.

Research focusing on the shaft resistance of piles includes the following. Shear tests of sand-pile interfaces have been performed to examine the effects of interface roughness [1, 2] and the stress change of the soil close to the pile due to soil dilation [3, 4]. Many centrifuge model loading tests have been conducted to investigate the vertical bearing capacity of piles in sandy soil [5-8]. In these tests, changes in the horizontal stress acting on the pile shaft were measured. The measured stress changes were found to be determined by the radial stiffness of the sand mass and the dilation of the shear band at the pile-sand interface. A series of shear tests of the pre-bored grouted planted pile were conducted to investigate the shaft capacity of pile-soil interfaces [9]. A numerical analysis using distinct element modeling (DEM) was performed to investigate shearing mechanisms at pile-soil interfaces [10, 11]. Furthermore, loading tests were performed to investigate the shaft resistance of piles in saturated and unsaturated soils [12].

On the other hand, the present study focuses on the shaft resistance of piles close to soil backfilled after the removal of existing piles. A previous study simulated the backfilling process for soil and conducted compressive loading tests on piles installed near backfilled sand columns [13]. Simulations of loading tests using the finite element method were also performed. The results show that if the conditions for the backfilled sand are different from those for the surrounding soil, the shaft resistance of the pile will depend on the density of the backfilled sand column and that the change in soil stress due to pile settlement will be different in the circumferential direction for the pile.

In this study, compressive loading tests were performed on a pile overlapping backfilled soil with different densities in a part of the surrounding soil to quantify the shaft resistance for the pile and the shear failure behavior of the soil adjacent to the pile. Several layers of colored sand were placed in the model soil to investigate the location of shear failure in the soil adjacent to the pile. After the loading test, the thickness of the shear band contributing to the axial resistance of the pile was determined based on observations of the deformation of the colored sand layer. In addition, a method for evaluating the change in horizontal earth pressure in the soil due to the settlement of the pile was investigated. Based on these results, a calculation method for the shaft resistance for the pile that considers backfilled soil was developed.

2. RESEARCH SIGNIFICANCE

The present study focuses on the shaft resistance for piles close to sand columns backfilled after the removal of existing piles. Specifically, the thickness of the shear band and the increase in horizontal earth pressure that contributed to the pile shaft resistance mechanism are investigated. The obtained data and findings will be useful for the design and risk assessment of pile foundations considering the effect of geotechnical uncertainties.

3. AXIAL COMPRESSIVE LOADING TEST OF PILE CLOSE TO BACKFILLED SOIL

Fig. 1 shows an outline of the experimental apparatus. The model soil is dry Tohoku quartz sand number 6, whose physical properties are shown in Table 1.

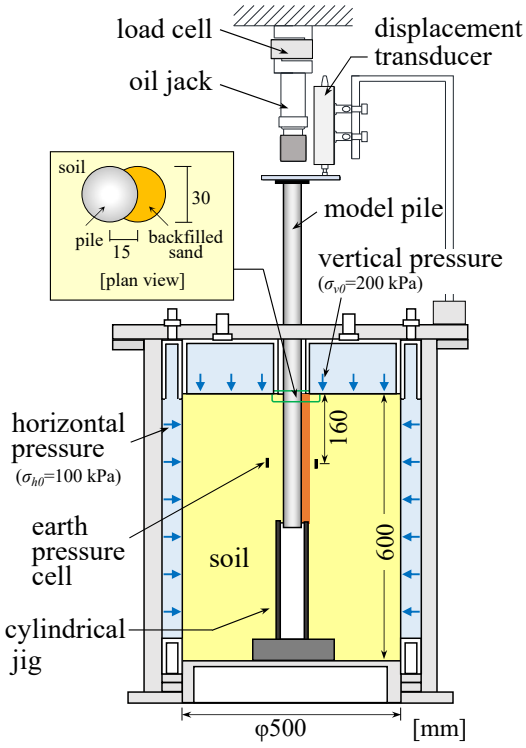

Fig. 1 Setup of experimental apparatus

Table 1 Physical properties of Tohoku quartz sand

Parameter	Value
maximum density, ρ_{dmax} (g/cm^3)	1.712
minimum density, ρ_{dmin} (g/cm^3)	1.397
mean grain size, D_{50} (mm)	0.32
coefficient of uniformity, U_c	2.3
coefficient of curvature, U_c'	1.3

The experimental construction process was conducted as shown in Fig. 2. The model soil was prepared at an arbitrary relative density using air pluviation in a cylindrical chamber. After 300 mm of sand was deposited in the chamber, a model pile was set up in the center of the chamber. The tip of the pile was inserted into a cylindrical jig to eliminate the tip resistance. At the same time, a crescent-shaped casing made from a copper plate with a thickness of 0.3 mm was placed next to the pile. This caused the pile to overlap the backfilled sand by half of the pile diameter. For the backfilled sand, sand of a predetermined relative density was deposited in the casing using a sand supply device [13]. The casing was pulled out according to the sand accumulation inside. During the preparation of the soil and backfilled sand, colored sand layers that were 2 mm thick were laid at 50 mm intervals. The heights and alignments of the layers are shown in Fig. 3. Finally, the model soil was deposited to a height of 600 mm. The effective embedded length of the pile on which the shaft resistance acted was 280 mm.

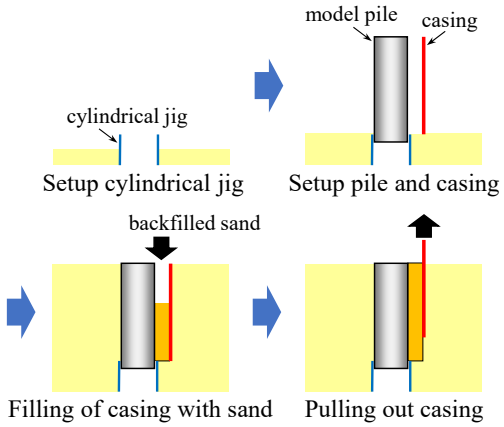

Fig. 2 Experimental construction process

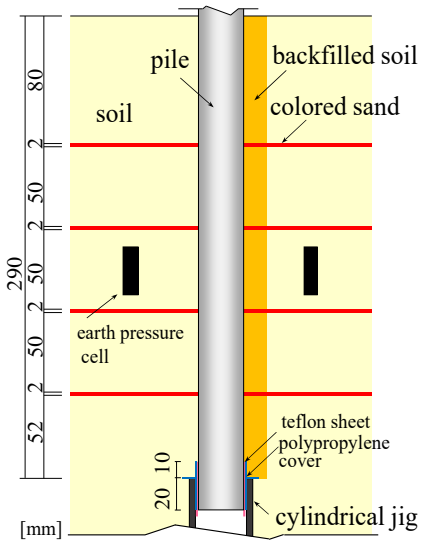

Fig. 3 Setup of colored sand

The model pile was an aluminum pipe with a diameter, d, of 30 mm and a thickness of 2 mm. The outer surface of the pile was roughened by a thermal spray coating (surface roughness of pile: R_{max} = 200 μm). Strain gauges were attached inside the pile at cross-sections G1 to G5 shown in Fig. 4 using a special long tool. The model pile was designed to be a closed-end pile to prevent damage to the strain gauges due to penetrating the sand into the pipe during loading tests and wetting the soil with water done after loading tests.

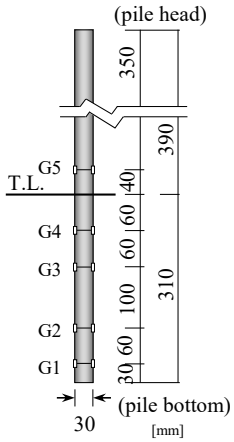

(a) Strain gauge locations

(b) Thermal spray coating

Fig. 4 Model pile

After the test specimen was prepared, a restraining pressure was applied to the soil through a rubber membrane by converting air pressure from a compressor to water pressure. The value of restraining pressure has a vertical pressure of σ_{v0} = 200 kPa and a horizontal pressure of σ_{h0} = 100 kPa.

A static axial compressive loading test of the single pile, in which a load was applied to the pile head using hydraulic pressure, was carried out.

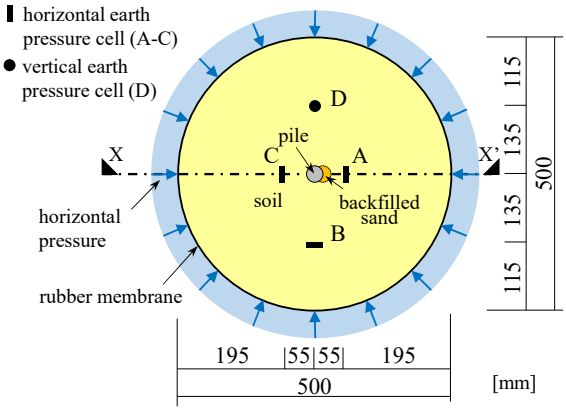

Fig. 5 Arrangement of earth pressure cells

Instrumentation was installed to measure the response of the pile during the loading test. A load cell and a displacement transducer were used to record the applied load and the displacement at the pile top, respectively. Strain gauges were attached to obtain the axial strain on the pile. Earth pressure cells were used to measure stress in the soil at the positions shown in Fig. 5.

The experimental variable was the relative density of the deposited sand. The test cases are shown in Table 2. The mechanical properties of the sand are shown in Table 3. The value of the internal friction angle of sand was obtained by direct shear tests under constant normal stress conditions. Three density conditions were set for the backfilled sand in the medium-density soil: low density (ML), medium density (MM), and high density (MD). In addition, two conditions, namely low density (LO) and high density (DO), of homogeneous soil with no backfilled soil were added for comparison. The hardness of the backfilled soil was considered by adjusting the filling sand to a predetermined relative density.

Table 2 Test cases

	LO	ML	MM	MD	DO
$D_{r,s}$ (%)	30	60	60	60	80
$D_{r,bs}$ (%)	-	30	60	80	-

*$D_{r,s}$, $D_{r,bs}$: Relative density of soil and backfilled soil, respectively

Table 3 Mechanical properties of sand

Relative density of sand, D_r (%)	30	60	80
Internal friction angle, φ (deg.)	29.3	32.1	34.9

*Cohesion of sand is almost zero.

4. RESULTS AND CONSIDERATIONS

4.1 Shaft Resistance of Pile

Fig. 6 shows the relationship between the shaft resistance of the pile and the settlement at the pile head. The value of f_s was calculated by dividing the axial force difference between the pile head and the pile tip (G1 in Fig. 4) by the pile circumference area in that section.

Regardless of the relative density of the soil, the maximum shaft resistance for the pile is reached around 2 mm ($\approx 6 \cdot D_{50}$) of settlement at the pile head. The displacement was required to mobilize ultimate shaft resistance along the model piles. The maximum value of shaft resistance (f_{smax}) depends on the density of the soil. The values of f_{smax} became in are those for LO, ML, MM, MD, and DO.

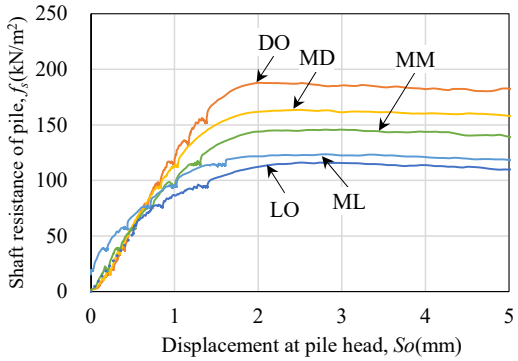

Fig. 6 Shaft resistance of pile versus displacement at the pile head

4.2 Earth Pressure

Fig. 7 and Fig. 8 show the relationship between the displacement at the pile head and the horizontal earth pressure. For LO, the horizontal earth pressure could not be measured when the displacement at the pile head was 0 to 0.5 mm. The horizontal earth pressure tends to increase until the shaft resistance for the pile reaches the maximum value. The soil near the pile caused expansion due to shear deformation of the soil.

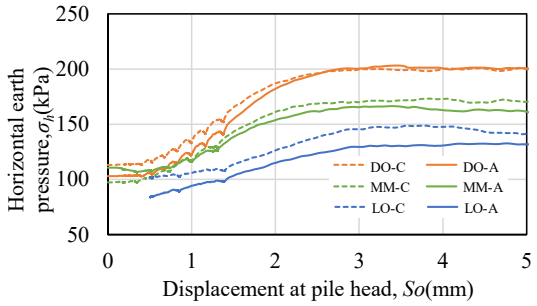

Fig. 7 Horizontal earth pressure at Z = –160 mm for LO, MM and DO

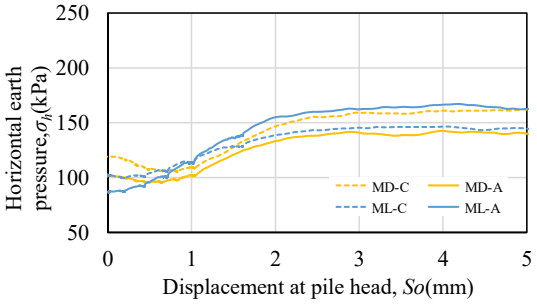

Fig. 8 Horizontal earth pressure at Z = –160 mm for ML and MD

4.3 Shear Band

After the compressive loading test of the pile, the soil was thoroughly moistened with water and cut longitudinally along the X-X' line in Fig. 5 through the center of the model pile and the backfilled soil. A stainless-steel plate with a cutting blade was used to cut the soil. Next, a scale was placed in close contact with the cut surface of the soil, and a high-resolution photograph was taken with a digital camera from the front of the cut surface, as shown in Fig. 9. The thickness of the shear band was measured as the distance from the outer surface of the pile to the point of alteration in the colored sand layer using the scale in the digital image.

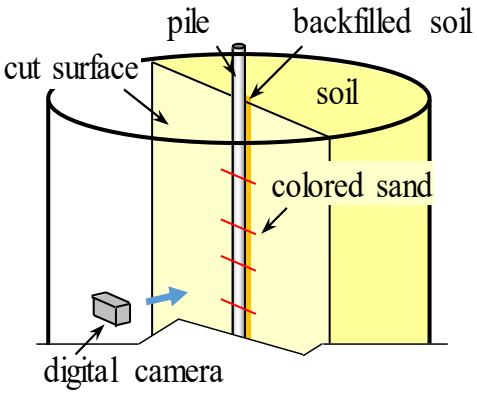

Fig. 9 Schematic diagram of observation of colored sand layer

Fig. 10 shows a cut section of the ML soil as an example, and Table 4 shows the average shear band thickness measured from the four colored sand layers. The shear band thicknesses for the homogeneous soil are LO < MM = DO. At the backfilled sand side (cell-A side) of the ML, MM, and MD, where backfilled sand with different densities is present, the shear band thickness is ML < MM < MD. It was found that the shear band became thicker as the density of the soil increased, but there was no correlation between the thickness variation in the depth direction. The shear band thickness ranged from 1.2 to 2.0 mm (3.8D_{50} to 6.3D_{50}). This value is closer to the results of Uesugi et al. (thickness of shear band $\alpha = 3D_{50}$ to $4D_{50}$) [14], who focused on the friction between steel and sand using a shear-type testing machine, than those of Nemat-Nasser et al. (thickness of shear bandα = 10D_{50} to 15D_{50}) [15], who used a hollow torsional shear test.

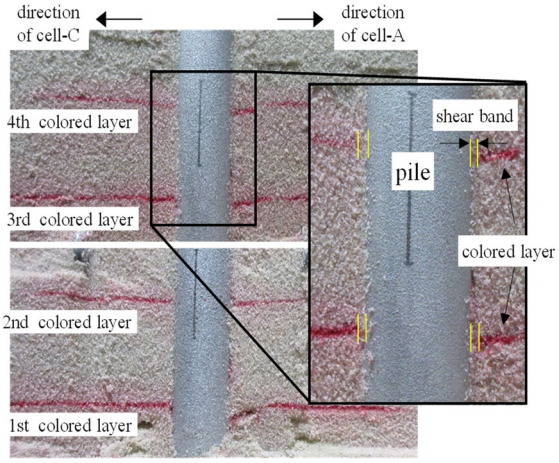

Fig. 10 Cutting surface of the soil in case of ML

Table 4 Measured thickness of the shear band

	LO	ML		MM	MD		DO
position	C &A	C	A	C &A	C	A	C &A
α (mm)	1.20	1.90	1.73	1.80	1.80	2.00	1.77

*α: distance from pile surface to shear failure

5. CALCULATION OF PILE SHAFT RESISTANCE CLOSE TO BACKFILLED SAND

The calculation of the shaft resistance for the pile close to the backfilled sand column is simply estimated by considering the thickness of the shear band and the change in earth pressure in the soil near the pile.

First, when the pile is subjected to compressive load, shear failure occurs in the soil near the pile if the outer surface of the pile is rough. The soil element adjacent to the pile is subjected to a mode of shear loading that involves stress rotation, and the major principal stress σ_1 and minor principal stress σ_3 for the soil element are inclined at about ±45° with respect to the vertical direction as shearing proceeds, as shown in Fig. 11 [16]. Shear failure of the soil element at any location is considered by applying the Mohr-Coulomb failure criterion. The shear stress τ_{rz} in the soil element at failure is expressed by

$$\tau = c + \sigma_h \cdot \tan\varphi' \quad (1)$$

where the parameter c is the sand cohesion, which in this study is 0 because the sand is dry. σ_h is the horizontal stress at the shear failure surface. The friction angle φ' is related to the internal friction angle of the soil element φ, and is given by [16]:

$$\varphi' = \tan^{-1}(\sin\varphi) \quad (2)$$

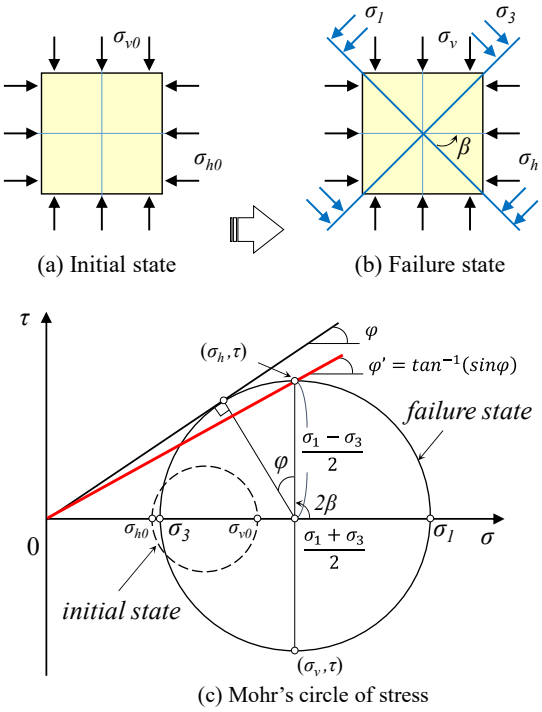

Fig. 11 Shear stress on failure plane in the soil near pile and Mohr-Coulomb failure criteria

The shape of the shear failure region in the soil and the backfilled soil adjacent to the pile is considered to be represented by the combination of two circles, as shown in Fig. 12, based on the results of numerical analysis in a previous study [13]. The values of α_s and α_{bs} are the thicknesses of the shear band in the soil and the backfilled soil, respectively. The values of θ_s and θ_{bs} are expressed in Eqs. (3) and (4), respectively, about the average value of α_s and α_{bs}.

$$\theta_s = \pi - \theta_{bs} \quad (3)$$

$$\theta_{bs} = \cos^{-1}\left(\frac{d+2\bar{\alpha}}{2d}\right), \quad \bar{\alpha} = \frac{\alpha_s+\alpha_{bs}}{2} \quad (4)$$

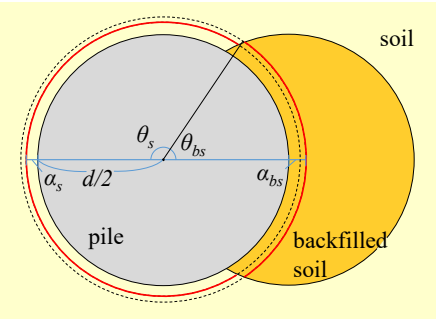

Fig. 12 Assumed shape of shear failure region

The horizontal earth pressure at the shear failure surface considers the increase in stress in the soil due to the expansion of soil elements, as shown in Fig. 13.

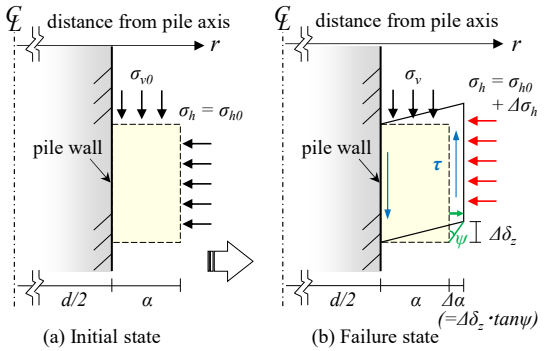

Fig. 13 Dilation and stress changes in the soil adjacent to the pile

The horizontal earth pressure is divided into three zones (A-C), as shown in Fig. 14. A previous study showed that as the earth pressure changes in the backfilled soil, the earth pressure in the soil on the opposite side of the backfilled soil also changes [13]. Therefore, when the stress changes due to volume expansion, the earth pressure is considered to be averaged so that the forces are balanced in zones A and C.

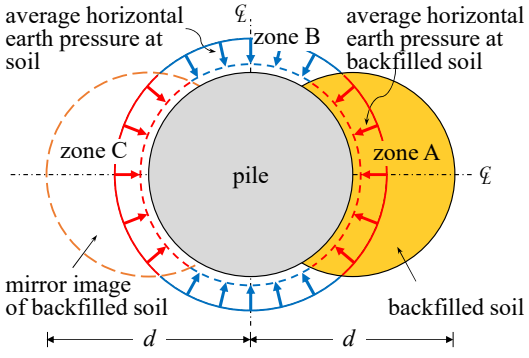

Fig. 14 Schematic diagram of earth pressure

The change in horizontal stress is evaluated by applying cavity expansion theory as shown in Eqs. (5) and (6) [7, 8, 17].

$$\sigma_h = \sigma_{h0} + \Delta\sigma_h \tag{5}$$

$$\Delta\sigma_h = \frac{4G}{d+2\alpha} \cdot \Delta\alpha \tag{6}$$

where G is the shear modulus of the soil or backfilled soil. $\Delta\alpha$ is the radial displacement at the soil or backfilled soil.

The radial displacement is expressed using Eq. (7). This displacement considers the radial deformation due to dilation as shown in Fig. 13.

$$\Delta\alpha = \delta_z \cdot \tan\psi \tag{7}$$

where δ_z is the settlement of the pile, and ψ is the dilatancy angle of the soil or backfilled soil.

The change in horizontal stress in zones A and C is calculated using Eq. (8).

$$\Delta\bar{\sigma}_h = \frac{\Delta\sigma_{h,s} + \Delta\sigma_{h,bs}}{2} \tag{8}$$

The location of the assumed failure surface differs between the shear stress due to the shaft resistance for the pile and the shear stress in the soil near the pile, as shown in Fig. 15. The shaft resistance of the pile f_s must be calculated by modifying the shear stress τ at the failure surface according to the thickness of the shear band.

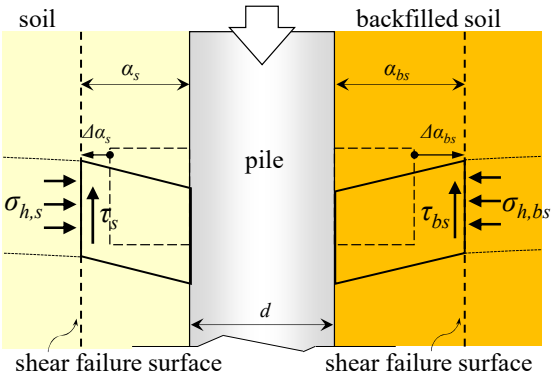

Fig. 15 Schematic diagram of shear stress and normal stresses in the soil adjacent to the pile

Based on the above, the shaft resistance $f_{s,cal}$ for the pile considering the shape of the shear failure surface can be expressed as

$$\begin{aligned} f_{s,cal} = & \frac{d+2\alpha_s}{d} \cdot \bar{\sigma}_h \cdot \tan\varphi_s' \cdot \eta \\ & + \frac{d+2\alpha_s}{d} \cdot \sigma_{h,s} \cdot \tan\varphi_s' \cdot (1-2\eta) \\ & + \frac{d+2\alpha_{bs}}{d} \cdot \bar{\sigma}_h \cdot \tan\varphi_{bs}' \cdot \eta \end{aligned} \tag{9}$$

where $\sigma_{h,s}$ and $\bar{\sigma}_h$ are the horizontal normal stress at the failure surface in the soil and the average horizontal normal stress between the soil and backfilled soil, respectively. φ_s' and φ_{bs}' are the friction angle of the soil and backfilled soil, respectively.

The ratio of shear failure of the backfilled soil to the total shear failure is evaluated by η, given by Eq.

(10), which depends on the length of the arc on the shear failure surface.

$$\eta = \frac{(d+2\alpha_{bs})\cdot\theta_{bs}}{(d+2\alpha_s)\cdot\theta_s+(d+2\alpha_{bs})\cdot\theta_{bs}} \quad (10)$$

A comparison of the pile shaft resistance between the above-mentioned calculation method and the experimental results was conducted. The initial shear modulus of sand was G_0 = 1.05×10^5 kN/m^2 which was determined to account for the applied restraining pressure level of the model sand based on the result of a soil test. The same value of the initial shear modulus was applied in numerical analysis in a previous study [13]. The shear modulus was reduced from 0.15 to 0.03 times the initial shear stress G_0 [8]. The value of G/G_0 was set at 0.12 in this study. The thickness of the shear band was determined by the values obtained in the experiment. The settlement of the pile, δ_z, was 2 mm.

Fig. 16 shows a comparison between the experimental values of the maximum pile shaft resistance $f_{s,exp,}$ and the calculated values $f_{s,cal}$ obtained using Eq. (9). Results from previous experiments [13] are also included in the figure. The value of $f_{s,cal}$ was evaluated to be about 10% smaller than the experimental value for ML, MM, and MD. The calculated and experimental values were almost identical for DO. The shaft resistance for the pile was evaluated to be about 30% smaller for LO. We believe that this is due to an underestimation of the earth pressure gauge measurements for LO. Based on the above results, we conclude that the proposed formula is applicable.

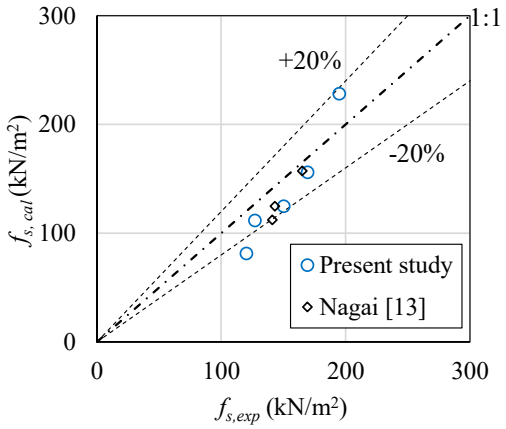

Fig. 16 Comparison of pile shaft resistance between experiment values ($f_{s,exp}$) and calculated values ($f_{s,cal}$)

6. CONCLUSIONS

The findings are summarized as follows.

(1) The thickness of the shear band in the soil adjacent to the pile increased with the increasing density of the backfilled soil. Its value ranged from 3.8 to 6.3 times the mean grain size of D_{50}.
(2) The change in horizontal earth pressure due to the pile settlement tended to decrease exponentially away from the pile. It was evaluated using cavity expansion theory.
(3) For the shaft resistance for the pile overlapped by backfilled soil, a calculation method that considers the thickness of the shear band and the shear failure of the sand separately in three regions was developed. It was found that the values obtained using the formula were about 10% smaller than the experimental values.

7. ACKNOWLEDGMENTS

The authors express their gratitude to the members of the research group at the Muroran Institute of Technology for gathering the data for this paper. This work was supported by the Japan Society for the Promotion of Science KAKENHI.

8. REFERENCES

[1] Uesugi M., and Kishida H., Frictional resistance at yield between dry sand and mild steel. Soils and Foundations, Vol. 28, Issue 4 1986 pp. 139-149.
[2] Uesugi M., Kishida H. and Tsubakihara Y, Friction between sand and steel under repeated loading. Soils and Foundations, Vol. 29, Issue 3, 1989, pp. 127-137.
[3] Boulon M., and Foray P., Physical and numerical simulation of lateral shaft friction along offshore piles in sand. Proceedings of the 3rd international conference on numerical methods in offshore piling, 1986, pp. 127-147.
[4] Tabucanon J.T., Airey D.W., and Poulos H.G., Pile skin friction in sands from constant normal stiffness tests. Geotechnical Testing Journal, Vol. 18, Issue 3, 1995, pp. 350-364.
[5] Fioravante V., On the shaft friction modeling of non-displacement piles in sand. Soils and Foundations, Vol. 42, Issue 2, 2002, pp. 23-33.
[6] White D.J. and Lehane B.M., Friction fatigue on displacement piles in sand. Géotechnique, Vol. 54, Issue 10, 2004, pp. 645-658.
[7] Lehane B.M. and White D.J., Lateral stress changes and shaft friction for model displacement piles in sand. Canadian Geotechnical Journal, Vol. 42, Issue 4, 2005, pp. 1039-1052.
[8] Lehane B.M., Gaudin C., and Schneider J.A., Scale effects on tension capacity for rough piles buried in dense sand. Géotechnique, Vol. 55, Issue 10, 2005, pp. 709-719.

[9] Zhou J., Gong X., Wang K., and Zhang R., Shaft capacity of the pre-bored grouted planted pile in dense sand. Acta Geotechnica, Vol. 13, Issue 5, 2018, pp. 1227-1239.

[10] Peng S.Y., Ng C.W.W., Zheng G., The dilatant behavior of sand–pile interface subjected to loading and stress relief. Acta Geotechnica, Vol. 9, Issue 3, 425-437, 2014.

[11] Zhou W.H., Jing X.Y., Yin Z.Y., and Geng X., Effects of particle sphericity and initial fabric on the shearing behavior of soil–rough structural interface. Acta Geotechnica, Vol 14, Issue 6, 2019, pp. 1699-1716.

[12] Fattah, M.Y., al-Omari, R.R. and Kallawi, A.M., Model studies on load sharing for shaft and tip of pile groups in saturated and unsaturated soils. Geotechnical and Geological Engineering, Vol. 38, Issue 4, 2020, pp. 4227–4242.

[13] Nagai H., Shaft resistance of piles close to backfilled sand columns. International Journal of GEOMATE, Vol. 21, Issue 84, 2021, pp. 121-128.

[14] Uesugi M., Kishida H. and Tsubakihara Y., Behavior of sand particles in sand-steel friction. Soils and Foundations, Vol. 28, Issue 1, 1988, pp. 107-118.

[15] Nemat-Nasser S. and Okada N., Radiographic and microscopic observation of shear bands in granular materials. Géotechnique, Vol. 51, Issue 9, 2001, pp. 753-765.

[16] Loukidis D. and Salgado R., Analysis of the shaft resistance of non-displacement piles in sand. Géotechnique, Vol. 58, Issue 4, 2008, pp. 283-296.

[17] Yu H.S. and Houlsby G.T., Finite cavity expansion in dilatant soils: loading analysis. Géotechnique, Vol. 41, Issue 2, 1991, pp. 173-183.